Environmental Health Perspectives
Vol. 84, pp. 57-73, 1990

Calcium Measurements with Electron Probe X-Ray and Electron Energy Loss Analysis

by Ann LeFurgey* and Peter Ingram†

This paper presents a broad survey of the rationale for electron probe X-ray microanalysis (EPXMA) and the various methods for obtaining qualitative and quantitatve information on the distribution and amount of elements, particularly calcium, in cryopreserved cells and tissues. Essential in an introductory consideration of microanalysis in biological cryosections is the physical basis for the instrumentation, fundamentals of X-ray spectrometry, and various analytical modes such as static probing and X-ray imaging. Some common artifacts are beam damage and contamination. Inherent pitfalls of energy dispersive X-ray systems include Si escape peaks, doublets, background, and detector calibration shifts. Quantitative calcium analysis of thin cryosections is carried out in real time using a multiple least squares fitting program on filtered X-ray spectra and normalizing the calcium peak to a portion of the continuum. Recent work includes the development of an X-ray imaging system where quantitative data can be retrieved off-line. The minimum detectable concentration of calcium in biological cryosections is approximately 300 μmole kg dry weight with a spatial resolution of approximately 100Å. The application of electron energy loss (EELS) techniques to the detection of calcium offers the potential for greater sensitivity and spatial resolution in measurement and imaging. Determination of mass thickness with EELS can facilitate accurate calculation of wet weight concentrations from frozen hydrated and freeze-dried specimens. Calcium has multiple effects on cell metabolism, membrane transport and permeability and, thus, on overall cell physiology or pathophysiology. Cells can be rapidly frozen for EPXMA during basal or altered functional conditions to delineate the location and amount of calcium within cells and the changes in location and concentration of cations or anions accompanying calcium redistribution. Recent experiments in our laboratory document that EPXMA in combination with other biochemical and electrophysiological techniques can be used to study, for example, sodium and calcium compartmentation in cultured cardiac cells. Such analyses can also be used to clarify the role of calcium in anoxic renal cell injury and to evaluate proposed ionic defects in cells of individuals with cystic fibrosis.

Introduction

Calcium has multiple effects on cell metabolism, membrane transport, and permeability and, thus, on overall cell physiology or pathophysiology. Electron probe X-ray microanalysis (EPXMA) has become established as a reliable technique where quantitative *in situ* determination of calcium content can be performed unambiguously. The determination is done on a cell-to-cell basis at the ultrastructural level by using thin, cryoprepared cells and tissues. The method is based on the physical interactions of electrons with matter at the atomic core shell level leading to the production of X-rays with energies that are characteristic of the elements comprising the specimen. These X-ray energies emanating from atoms provide highly specific information about the atoms but do not distinguish between species or between bound and free forms of the element, measuring, for example, total calcium rather than free Ca^{2+}. Somlyo has reviewed some of the limitations and applications of EPXMA for measurement of calcium (*1*). The complementary technique of electron energy loss spectroscopy (EELS) has been used less often, primarily because analyses must be performed on extremely thin (< 60 nm) uniform sections of tissue. However, Shuman and Somlyo have successfully applied EELS to quantitate very low levels of Ca in some cell systems (*2*). For comprehensive detail on electron probe microanalysis methodology, the reader should refer to numerous texts and textbooks (*3-14*). In this introduction we summarize the principles and practical techniques involved, and provide some recent data on quantitation and imaging.

*Division of Physiology, School of Medicine, Duke University, Durham, NC 27710.
†Research Triangle Institute, Research Triangle Park, NC 27709.
Address reprint requests to P. Ingram, Research Triangle Institute, P.O. Box 12194, Research Triangle Park, NC 27709.

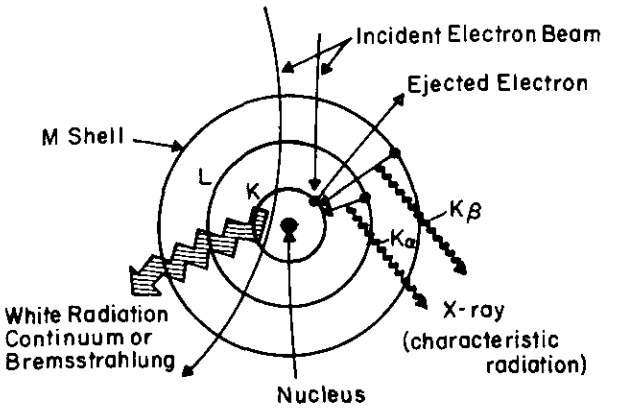

FIGURE 1. Schematic illustrating the producton of X-rays by inner atomic shell ionization (characteristic radiation) and nuclear scattering (continuum radiation).

Physical Principles of X-Ray Spectrometry

When inelastic scattering takes place through the interaction of electrons with the atomic nucleus (Fig. 1), the electrons lose energy when crossing through the Coulomb field of the nucleus, and in doing so, they lose energy over a wide spectrum of the energy range. The X-rays generated are the so-called white radiation or bremsstrahlung radiation (breaking radiation), which forms the continuous background over which all other (characteristic) X-ray signals are superimposed (Fig. 2). The presence of this continuum radiation can be used as a direct measure of the mass-thickness of the sample (see sections on quantitation).

When, however, the electrons interact with the inner orbital electrons in the K, L, or M shells, some of these electrons are ejected, leaving a hole in that particular shell. According to quantum theory, this hole must be filled by an electron from a shell of higher energy. This transition results in the emission

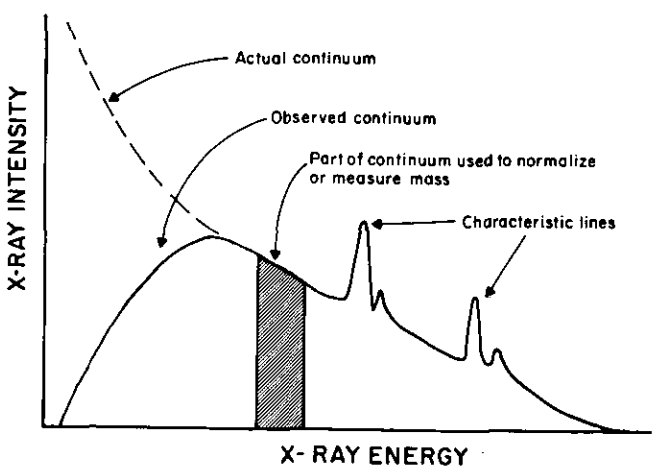

FIGURE 2. Typical energy dispersive X-ray (EDX) spectrum of characteristic peaks superimposed on a broad continuum (solid line). The dotted line represents the shape of the continuum if there were no absorption of X-rays by the beryllium window of the detector and self-absorption of the sample.

of X-ray radiation with a characteristic energy that is equivalent to the binding energy of the shells. For example, the element calcium will have at least two detectable peaks—a K_α and a K_β involving transitions from the L and M shells , respectively. Higher atomic number elements have many more shells and subshells and give rise to a plethora of emissions that can lead to severe peak overlap problems (*3*).

The mechanism of X-ray detection is discussed in some detail since techniques for their measurement have become the most widely established in microchemical microscopy. However, it is important to note that there are many other physical processes at work that provide analytical information (such as Auger electrons and cathodoluminescence). The electrons, which have lost their energy because of the ionization process responsible for these events, can also be detected and measured; EELS has been hailed as an extremely powerful technique for identifying different elements in biological thin sections (*2, 15–20*). While it is true that EELS is a nonfluorescent and efficient process (unlike X-ray spectrometry), it has been used only occasionally for conventional tissue examinations and is still fraught with technical difficulties. Thin sections for EELS must routinely be cut at ≤ 60 nm, and only low atomic number elements ($Z < 30$) can be detected with optimum sensitivity. However, EELS is a powerful research tool that can provide detailed information on the interaction of electrons with the sample and subsequent image formation of isolated biological macromolecules, frozen suspensions of proteins, and frozen thin sections of tissues. An additional biological application is the use of zero loss EELS to measure the total mass in frozen, hydrated sections of tissues (*21*), thus enabling a direct calculation of wet weight concentrations of calcium and other elements in subcellular compartments.

Both the wavelength and energy of X-rays can provide highly specific information about the atoms where the X-rays emanante, but usually they cannot distinguish between species (e.g., Fe_2O_3 or Fe_3O_4). A wavelength spectrometer analyzes the wavelength of the X-rays using classical crystallography (based on Bragg's law). With energy dispersive X-ray (EDX) microanalysis, the energy of the X-rays is detected and measured.

The major advantage of wavelength dispersive X-ray (WDX) microanalysis is that usually one obtains a better peak-to-background ratio, thus the sensitivity can be greater. However, in order to achieve this better peak-to-background ratio, large beam currents or very long counting times are necessary. Often these beam currents are so great that they severly damage a biological sample. Furthermore, with WDX it is necessary to scan specifically for a single element at one time. With EDX, one simultaneously obtains characteristic peaks from all elements in the sample generally with those having an atomic number of 9 (fluorine) or greater. (WDX can be used for atomic

number elements somewhat lower, e.g., down to lithium.) Thus, with EDX one can quickly scan a sample in order to see what other elements may be present.

On reflection, this unique feature of EDX microanalysis is unusual in analytical chemistry. Ordinarily, it is necessary to look for a specific element with a specific window, for example, as used in atomic spectroscopy. With EDX, even if the investigator has no inkling that a given element might be present, the spectrometer will reveal its presence as a characteristic peak. In general, an EDX spectrometer is more useful for biologists than a wavelength spectrometer and would be recommended as the first choice. Certainly in biomedical applications an energy dispersive spectrometer is clearly the most useful instrument. Nevertheless, the reader should be aware of the work by Fiori et al. (*22*) and Lechene et al. (*23-25*) using WDX. The former were able to demonstrate localization of aluminum to neurons in the hippocampus in some samples. It is unlikely that they could have generated these maps with energy dispersive techniques, since the peak-to-background ratios were unfavorable for aluminum. WDX has become most useful in the systematic examination of small (< 1 μL) droplets of urine (*24*) for example, and single cells from culture (*25*). Thus, there clearly are applications of WDX in biology that are extremely important, but are not within the scope of this article.

X-ray photons behave in much the same way as other types of electromagnetic radiation; that is, they have wavelength and energy that are inversely related. As noted above, one can analyze either property in order to determine which elements have given rise to them.

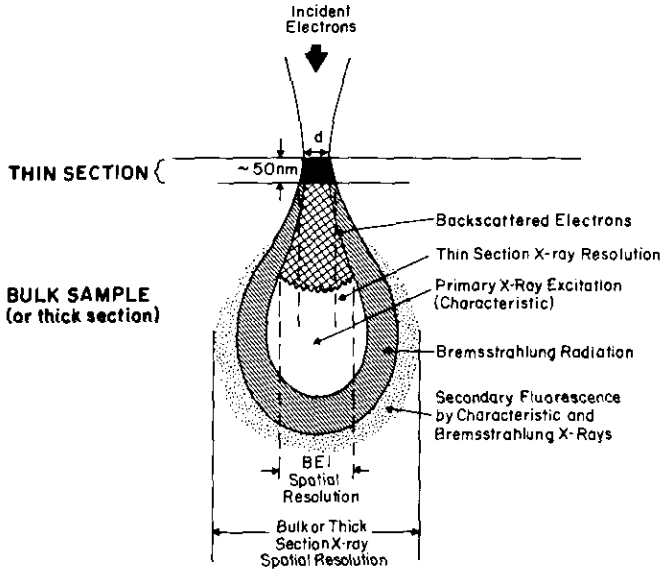

FIGURE 3. Schematic of the electron interaction volume in a solid of medium-to-low atomic number. The improved spatial resolution resulting with thin sections is evident.

Figure 3 summarizes the physical effects of the scattering processes within a material. The scattering process, by definition of the term, will result in an activated volume within the sample that is considerably greater than the dimension of the beam that is impinging on it. Although the shape of the volume shell will vary according to the atomic number of the material and the accelerating voltage of the electrons (the lower the voltage, the less pear-shaped and more spherical it is), it can be seen that for optimum spatial resolution, one would like to use thin sections and higher voltages. It is important, therefore, for the biologist to realize that EDX microanalytical resolution can be improved by microtomy. By removing the bulk portion of a sample and only studying a thin slice, many of the problems of poor resolution illustrated in Figure 3 are solved. Nevertheless, the act of ultramicrotomy can itself produce artifacts. However, EDX microanalysis on bulk material has been used successfully for several important problems in biology.

For example, many lung particulates fall into the 1 to 10 μm range and are easily detectable in a relatively inexpensive, conventional scanning electron microscope that is equipped with an EDX spectrometer. Marshall (*26*) has successfully studied the composition of fluids in gland lumens using bulk EDX techniques. It would be difficult and probably impossible to obtain data on a large fluid space such as a gland lumen using thin sections. The instrumental configuration that may be used is shown schematically in Figure 4 where the specimen may be either a thin section as shown, a deparaffinized section such as that used for light microscopy, whole tissue or individual cells.

Instrumentation for High Resolution Analytical Studies

A conventional, high resolution transmission electron microscope (CTEM) may have a separate scanning system and energy dispersive X-ray microanalyzer added to it (Fig. 5). The basis of operation of any scanning electron microscope is that a small focused beam of electrons is rastered, in some fashion, across the sample and the appropriate signal—whether it be transmitted electrons, X-rays, or other electrons—is appropriately converted to an electrical voltage with a suitable detector. That voltage is then displayed on a cathode ray tube as an intensity modulated spot that scans in synchronization with the electron beam itself. If X-ray probing is done with a CTEM where electron optics that are similar to the optics found in the light microscope are operative, the beam may also be focused to a small but stationary spot on a small area of interest of the sample. By either focusing the spot to a small size with suitable condenser apertures or placing a selected area aperture in the electron column, the regions for electron diffraction may be probed and

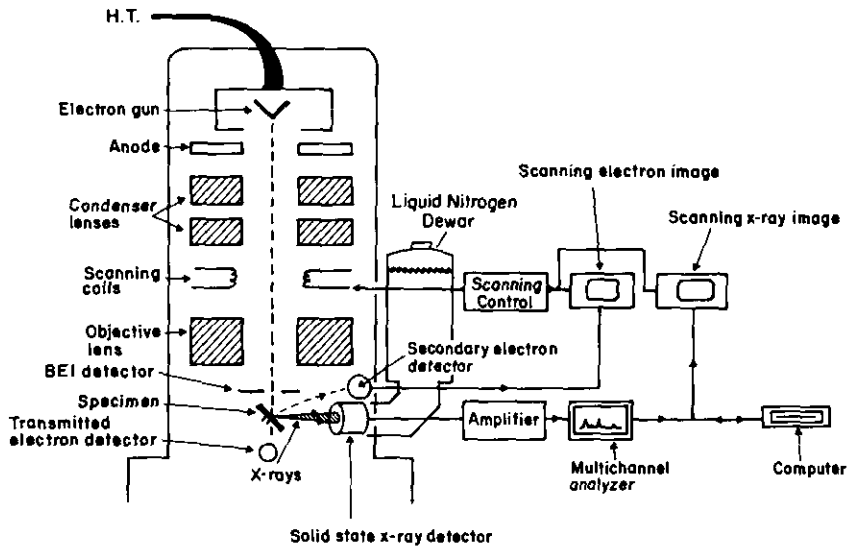

FIGURE 4. Schematic diagram of a simple scanning electron microscope equipped with backscatter, transmitted electron, and EDX instrumentation.

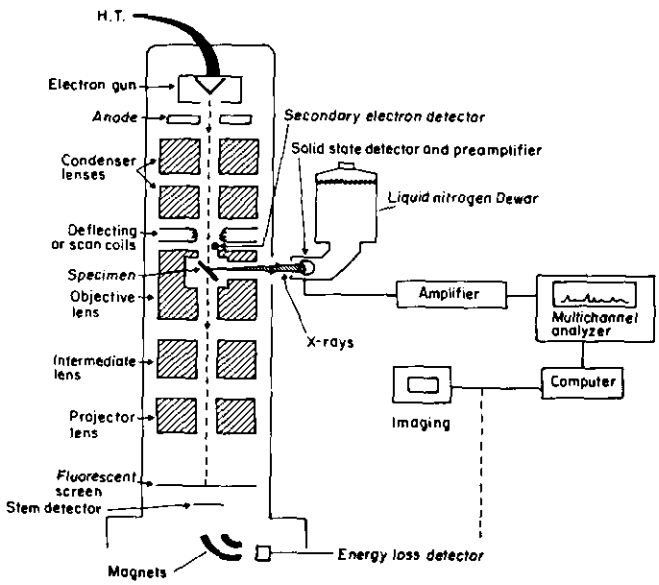

FIGURE 5. Schematic diagram of a conventional transmission electron microscope equipped with EDX and energy loss facilities. Such an instrument is usually referred to as an analytical electron microscope (AEM).

visualized at the same time. In the case of a scanning system where the size, shape and orientation of the image raster may vary, the size and shape of the electron beam may be altered by varying the astigmatism to provide coverage of just the area of sample that is being probed (27). Figure 5 also shows what has come to be known as an analytical electron microscope.

A typical EDX system is composed of a single crystal of silicon between 10 and 30 square mm in area that has been doped with a small quantity of lithium. When a charged particle impinges on the crystal, an electron-hole pair is formed (Fig. 6). The magnitude of this pulse of charge generated is proportional to the energy of the particle (in this case an X-ray photon) and is collected by an application of high voltage through thin gold electrodes across the crystal. The charge pulse is then converted to a voltage with a charge sensitive preamplifier known as a field effect transistor (FET). The pulses are suitably amplified, processed, and stored in an appropriate number of voltage bins in a multichannel analyzer or computer memory. These voltages can then be displayed on a cathode ray tube or X-Y recorder as peaks corresponding to the energy of the original X-ray photons. The detector and pre-amplifier (FET) are generally kept in a light-tight enclosure to prevent non-X-ray photons from exciting the Si(Li) crystal and also at liquid nitrogen temperatures, in order to reduce electronic noise and prevent charge recombination in the Si(Li) crystal.

The dewar-encased system, containing about 7 L of liquid nitrogen, is attached to the electron column (as shown in Figs. 4 and 5) with the detector placed as close to the sample as possible. This system is usually separated from the microscope vacuum by a very thin (about 8 μm) beryllium window. In addition to protecting the Si(Li) crystal, this window excludes both low energy X-rays and most backscattered electrons,

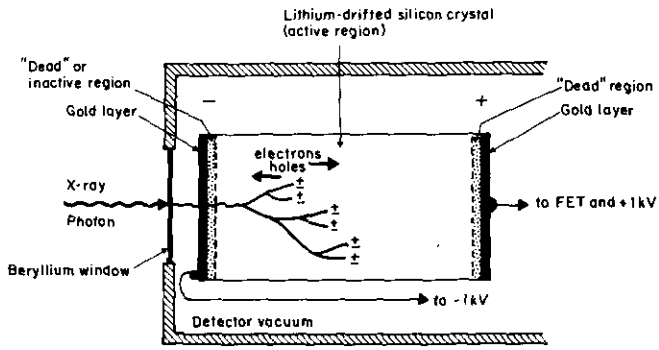

FIGURE 6. Schematic diagram of a Si(Li) detector used for EDX.

as charged particles could also elicit a response from the detector. At higher accelerating voltages, these backscattered electrons appear as a continuous background superimposed on the bremsstrahlung continuum, and they have to be subtracted out in any quantitative measurements that are made. (They can be eliminated in some cases by placing a magnetic electron trap in front of the detector.) The cut-off of low energy X-rays usually means that most detectors can only reliably detect X-rays with the energy of about 1 keV (i.e., sodium) and above, and the sensitivity to elements such as sodium and magnesium is reduced. (Occasionally, fluorine has been detected with this kind of detector.)

So-called windowless or ultrathin window detectors have been used in microprobe analysis to detect the presence of carbon, oxygen, and nitrogen. At present, they are of limited applicability in routine situations because one is not primarily interested in the quantitation of carbon, oxygen, and nitrogen.

In addition to the lower fluorescense efficiency of X-rays from low Z elements, the presence of a beryllium window absorbing the low energy X-rays results in a much reduced sensitivity to elements such as sodium and magnesium. A typical X-ray spectrum from a section of necrotic tissue is shown in Figure 7. Although the actual sodium to potassium ratio in this tissue is about 10 to 1, the apparent peak-to-backgrounds of the two peaks are approximately the same. Conversely, at high X-ray energies (>15–20 Kv) the quantum efficiency of the Si(Li) detector will fall off because some of the X-ray photons will pass through the crystal without producing electron hole pairs.

Analytical Modes

In EPXMA one can take advantage of electronic imaging in a sequential or digital fashion and also the ability to manipulate the contrast the signal of interest to the optimal extent, either with analog electronics or with a computer. However, there are four basic modes of instrument operation with EDX: fixed spot, raster, line scan, and X-ray imaging.

In the spot mode the beam is kept in a fixed position and a fixed size that is determined by the lens settings of the microscope. Either the specimen is moved manually or by computer control, or the beam itself is similarly moved in order to obtain a signal from a specific region of the specimen. A spot mode also has the advantage that all the electrons are concentrated into a small area; the disadvantage is that the specimen may drift during analysis, although there are now computer programs to correct for this.

The raster mode can be used either to get a general overview of the elemental constituents of a specimen. By using high magnification and a small raster one can probe regions of interest at known magnifications, while simultaneously viewing them. (This process can be of use if one suspects there might be some slight sample drift.)

The line scan mode is essentially the formation of a one-dimensional image, i.e., the spot is scanned in a single line across the sample containing regions of interest. By feeding the X-ray signal from any element into the scanning electron microscope amplifier, a line profile specific to the element of interest is obtained on the scanning electron microscope screen. Thus, one can confirm spatially the presence of a particular element in graphical form. (This modulated line can also be rastered to form a two-dimensional X-ray image.)

The logical extension of this is to take that same X-ray signal and feed it into the scanning electron microscope (SEM) amplifier instead of modulating a line in the Y direction, modulate the spot on the cathode ray tube of the SEM. A so-called, "dot map," is formed, corresponding precisely to the spatial distribution of the element of interest from the X-ray spectrum. In the case of sections, a variation in thickness could cause possible X-ray image artifacts. In any of these analyses it is mandatory to select a region from the X-ray spectrum that is devoid of characteristic peaks and in the bremsstrahlung region, and then form an image with this region to verify the positivity of the suspected characteristic X-ray. Of course, it is also possible to make maps of several elements present at the same time; this is of value particularly if one is able to make multicolored images and build up a montage of elemental distributions within the sample.

Dot maps were an early form of X-ray imaging, for which it was difficult to extract quantitative elemental data without measuring the coordinates and energy of each dot. The maps are more or less qualitative where one dot corresponds to the detection of one specific X-ray photon by the detector.

A much more satisfactory technique, which can be quantitative (see section "Quantitative X-ray Imaging") as well as qualitative, is to form the element-specific X-ray image picture-element by picture-element (pixel by pixel), where the electron beam is stationary for finite periods of time and where it can be controlled digitally at all times during the scan (*28*).

Most X-ray spectrometers can function, in part, as the digital imaging portion of a microscope. This enables images (of any type) to be processed much more effectively with a computer, which is an integral part of every commercial X-ray system today.

Qualitative Elemental Identification

While the presence of most element peaks is unequivocal, given a reasonable peak to background ratio (> 1-2), it is clear that from the number of possible transitions from one orbital shell to another, severe peak overlaps can occur. These must be appreciated so that erroneous conclusions will not be drawn from the data. The appropriate choice of grid materials (e.g., copper or nickel) should be made such that overlaps

from sodium or tungsten, for example, do not interfere with the spectral data. A particularly serious overlap involves the potassium K_β and the calcium K_α peak at 3.59 and 3.69 keV, respectively. Sophisticated computer programs are essential for deconvolution of the peaks, especially for detecting small amounts of calcium in the presence of high potassium. Accurate calibration and electronic stabilization of the spectrometer and detector are essential in order to obtain reliable quantitative data (see section "Quantitation: Calcium and Other Elements").

Consideration must be given to the artifactual or background peaks due to stray radiation from metals in the instrument such as iron, chromium, nickel, etc., which are common problems in many analytical electron microscopes. In addition, lines for silicon and sulfur may arise from contaminating vacuum pump oil (possibly on the cold surface of the detector windows), o-rings, and instrument parts. Because of charge build-up effects in the detector, it is often possible to detect a spurious peak at the excitation energy of silicon (the detector material), or at the peak energy minus 1.72 keV, the so-called, "escape peak". For example, in the case of a large calcium oxalate inclusion in a kidney nephron section, a spurious peak can be found at approximately 1.90 keV that overlaps almost totally with phosphorus, thereby leading to a possible erroneous conclusion. In fact, it is not calcium phosphate that has formed, but calcium oxalate. Conversely, in the presence of very strong peaks, arithmetic doublets can be formed. For example, in the case of silicon contamination (as mentioned above), the doublet of silicon is 1.72×2 or 3.44 keV, which occurs exactly in the potassium/calcium region, again leading to a possible erroneous identification.

The peak width or energy resolution is the direct result mostly of the statistical distribution in the generation of charge carriers by the X-rays impinging on the Si(Li) crystal. Also, it is partly the result of electronic noise in the amplifiers. The peak width is somewhat energy dependent (worse for higher atomic number elements) and is usually rated on a detector, as about 150 eV at 5.9 keV, the manganese K_α peak.

Most modern-day spectrometers have a built-in computer program for checking these parameters. [The inherent width of an X-ray peak is about 2 eV at 5.9 keV. Wavelength dispersive spectrometers have much better peak resolutions (approximately 10 eV) than EDX spectrometers, and thus they have better peak/background ratios and few peak overlaps.]

Spurious peaks and their spectral artifacts can sometimes arise from improperly grounded circuitry and vibrations (microphonics) in the detector or liquid nitrogen dewar (moisture accumulation in the form of small ice particles). Care must be exercised on installation to eliminate such problems.

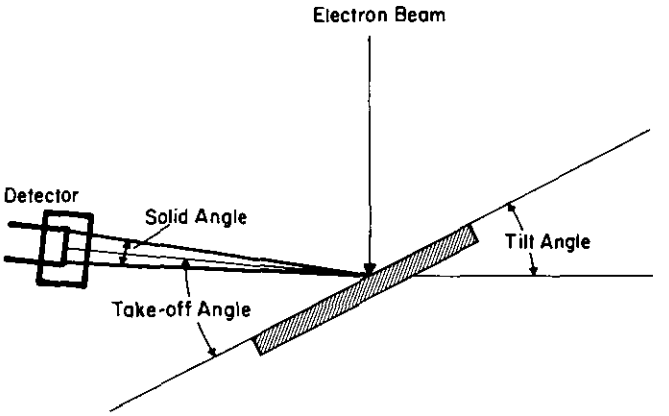

FIGURE 7. Diagram showing relationship between tilt, take-off, and solid angles in an AEM.

Quantitation: Optimal Instrument Operation

In many physiological or pathophysiological instances, one is dealing inherently with very small concentrations of calcium and other elements (in the millimolar range); therefore, the optimization of the microscope and detector parameters is vital. Since all microscopes are not built equally, knowledge of these parameters can be quite important. For example, the solid angle (Fig. 7), subtended by the detector surface to the specimen, is of crucial importance in determining sensitivity. In a typical TEM, however, the solid angle is at best only about 0.14 steradians for a side-entry X-ray detector, and it is about an order of magnitude less for the normal top-entry detector. Therefore, in the case of the examination of thin biological specimens in a TEM, it is usually better to choose the side-entry configuration.

Quantitation is affected by the choice of accelerating voltage. Since atomic cross-sections vary from element to element, the efficiency of X-ray generation is not the same for all elements at any one accelerating voltage. For any one element, the ionization cross-section (which is directly related to the intensity of X-rays generated) is highly dependent on the ratio of accelerating voltage to the absorption edge energy (sometimes called the "overvoltage"). The optimum efficiency of excitation of any one shell element is approximately three times the overvoltage (*14*). However, balanced against this is the bremsstrahlung equation, which states that the higher the voltage, the less the specimen bremsstrahlung because the cross section of the material is far less (*29*). Consequently, the peak-to-background ratio (P/B), which turns out to be the crucial parameter for determining concentrations, generally tends to increase with increasing voltage, but not in a linear fashion (*30*). This will apply mainly to thin sections.

One also must optimize the tilt of the specimen towards the detector to optimize the take-off angle, with the knowledge that the geometry of the region to be examined will be affected (Fig. 8). As mentioned

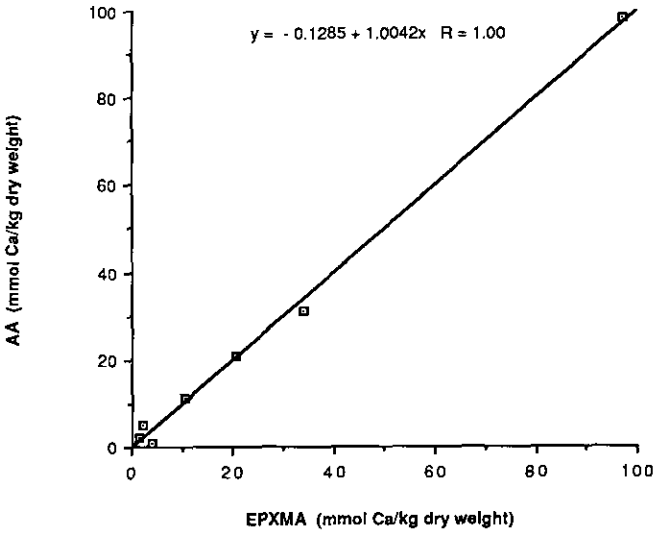

FIGURE 8. Calcium concentration measured in bovine serum albumin by EPXMA against atomic absorption (AA).

earlier, care has to be exercised in identifying extraneous sources of X-rays from instrument parameters such as pole pieces, grid bars, and even X-rays fluoresced from adjacent regions of specimens. An understanding of these paramenters is necessary before embarking on any form of quantitation (*31,32*). In the TEM mode, particularly, specimens need to be examined near the center of a grid square. If the sample is too near the grid bar, it can mask spectra. One also has to guard against characteristic radiation from the above-mentioned components as well as bremsstrahlung.

The EDX electronics must be set optimally for the low count rates that are generated from biological specimens. All EDX electronics essentially count and sort pulses. Electronics can only handle pulses at a certain rate that is rather low (< 3000 counts/sec). However, most commercially available EDX systems are sold for a wide variety of uses—one which may include acceptance of very high count rates. Therefore, the systems possess built-in pulse shaping electronic and storage devices so that if the count rate is too high, the X-ray pulses are stored for a certain period before the electronics can continue counting (so-called "dead time"). Dead time can also seriously affect the sensitivity of the system. However, since most biological specimens can be probed consistent with a beam current high enough (~10^{-9} amps) to yield reasonable count rates (a few hundred/sec) from an acceptable probe diameter (10 to 100 nm), the electronics can easily be set to count optimally with a dead time of ≤ 30% to provide quantitative accuracy. A well cryo-trapped, clean, baked-out microscope is necessary for consistent quantitative EPXMA. Generally, the use of a clean, cold stage is preferred in order to minimize radiation effects on the sample (*27, 32–34*).

Quantitation: Calcium and Other Elements

In high resolution studies the most commonly used quantitative algorithm is continuum normalization, a technique developed by Hall and colleagues (*35–42*) that is based on the premise that continuum X-ray intensity gives a measure of local total mass of the analyzed volume. Since the intensity of a peak characteristic of the excited atoms' energy is proportional to the mass, the concentration is simply the ratio of the elemental peak intensity to the continuum intensity.

The continuum method has been refined by Somlyo, Shuman and colleagues (*27,43,44*) to include digital filtering for background removal and multiple least squares fitting to peaks from suitable standards Calibration can be checked by comparison with other analytical methods such as atomic absorption spectrometry (Fig. 9). Other methods such as those using standards sectioned together with the tissue (*45*) are less reliable due to local inhomogeneities in section thickness.

In the special case of the physiologically important element calcium, EPXMA has been extended to its practical limit of sensitivity by Bond et al. (*46,47*). They were able to detect 300 μmole Ca/kg dry weight in the cytoplasm of cryosectioned smooth muscle cells. Measurement of Ca in most biological systems is difficult because *a*) in an X-ray energy spectrum, the K K_β peak overlaps the Ca K_α peak, and *b*) relatively miniscule amounts of Ca occur in conjunction with large amounts of K. Because of this overlap, significant errors can occur unless both the peak centroid position and peak resolution are maintained between reference standards and sample. Shuman et al. have shown that a 4 eV shift in peak calibration can yield a 30% error in measuring the Ca content. Kitazawa, Somlyo, and Shuman (*43*) incorporated the first and second derivatives of the K X-ray peaks in a multiple least squares fitting routine to correct for changes in calibration. With this method they measured 1 ± 0.2

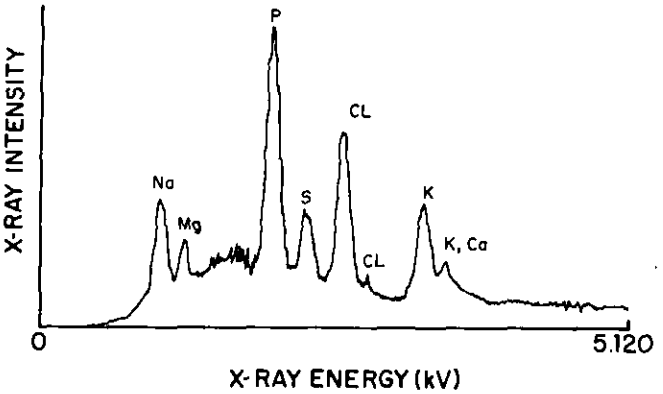

FIGURE 9. Typical EDX spectrum from necrotic tissue illustrating the severe overlap between potassium K_β and calcium K_α peaks. Although the sodium and potassium peaks are about the same size, the Na/K ratio is about 7:1 as a result of the effects shown in Figure 2.

mmole Ca/kg dry weight in the presence of 500 mmole K/kg dry weight.

Environmental Ca contamination in any form also must be eliminated during specimen preparation. Also the extension to a sensitivity of 0.3 mmole (300 μmole) Ca/kg dry weight requires long collection times and a large number of spectra (300–500 sec/spectrum, 30 hr total counting time).

Since the X-ray counting process is highly inefficient (~1%) and follows Poisson statistics and, thus, the square law, doubling sensitivity requires one to quadruple counting time (or increase beam current). Quantitation of Ca is significantly easier and less time consuming at higher Ca content levels (approximately 100 mmole/kg dry weight) or lower K levels (< 100 mmole/kg dry weight). These criteria are met, for example, in the terminal cisternae of skeletal muscle under control conditions and in cell cytoplasm or mitochondria after experimental treatment with Na-K-ATPase inhibitors. Experimental determinations of minimum detectable concentration for most other elements of physiological interest are in the range of approximately 1 mmole/kg dry weight.

Quantitative X-Ray Imaging

Images, in general, can be formed by two fundamental processes. All the pixels are either created simultaneously (as in a conventional light or electron microscope), or they are formed sequentially (as in a scanning confocal light microscope, scanning electron microscope, or television set). Since X-ray generation is a statistical process and X-rays cannot be focused by lenses, the latter method is used for quantitative X-ray imaging. The electron beam dwells for a finite period of time at each pixel where a complete X-ray spectrum is collected and processed by a computer (*28,48–56*) (Fig. 10). By arranging the pixels in a matrix and building up the image line by line, reproducible and fully quantitative images of all the elements of interest can be obtained (Fig. 11) (*50*). However, with a dwell time of 1 sec per pixel and allowances for processing, a 64 × 64 pixel image takes about 2 hr to acquire.

To obtain better counting statistics, especially for the low levels of calcium often encountered in physiologically normal cells, it is necessary to dwell for several seconds per pixel. To obtain better spatial resolution, the matrix resolution must be increased to 128 × 128 or even 256 × 256. Thus, acquisition times can be long (up to several days), but all the elemental information, including the continuum, standard deviations, and chi-squares (goodness of spectral fitting) can be gathered and stored for later display and image processing.

The result is that this method is far more efficient than collection of data at each point from an electron microscope image. If the final X-ray image does not show good enough statistics in any area, it can always be subsequently probed in a static mode for a longer time (*28*). A second advantage of quantitative X-ray imaging is that a perception of the distribution of calcium and every other element is obtained. This can be invaluable in assessing the overall condition of the sample (see section "Applications in Cell Physiology"). Third, as will also be seen below, the best cryopreserved specimens often show little or no discernable morphology. It is *only* after elemental imaging that one can appreciate the ultrastructure, i.e., true microchemical microscopy! Finally, because of the long acquisition times involved in collecting an image, there will inevitably be some sample (image) drift. This can either be corrected *post facto* (*53,57*) or on line during acquisition (*58,59*).

From the point of view of spatial resolution, the limitation will be a function primarily of the electron probe size, as well as the atomic cross-section of the material itself. Multiple scattering into the pear-shaped distribution of X-rays can be reduced by cutting thinner sections of tissue (about 50 nm is the practical limit). However, increasing the probe current to obtain statistically better images also increases the probe diameter, thus worsening the resolution. Generally, with beam currents in the 10^{-9} amp range, good resolution is obtained for calcium at about 10 to 20 nm. Any improvement on this probably requires the use of a field emission (cold cathode) electron source, as has been demonstrated by Somlyo and colleagues (*48*); they were able to obtain resolutions of approximately 8.9 nm from thin catalase crystals.

If sample preparation difficulties can be overcome, elemental EELS holds the potential for better spatial resolution than EPXMA. This is because EELS is not a fluorescent process and, in principle, uses almost all the electrons involved in formation of a normal electron image. Shuman (*2*), Leapman (*18*) and colleagues have shown that it is possible to quantitate and image levels of Ca down to about 200 μmole/kg dry weight.

Electron Energy Loss Spectroscopy

As noted in the second section, electrons that have lost energy by virtue of their interaction with the atomic core shells can have their energies measured in order to identify and quantify the prevalence of the elements that have given rise to the losses. This can be done by either using a magnetic sector spectrometer (*2*) or a prism filter (*17*) judiciously placed so as to collect and/or image the electrons traversing the specimen (Fig. 5). Without discussing the merits of either method, most of the quantitative data to date has been obtained from some form of photoelectric camera/counter placed directly behind a slit where the spectrum can be scanned (serial collection) in a magnetic sector instrument.

Parallel detectors using diode arrays are now available which greatly increase the efficiency of collection. As in EDX instruments, data can be processed in a multichannel analyzer. However, special processing techniques are required since the main analytical

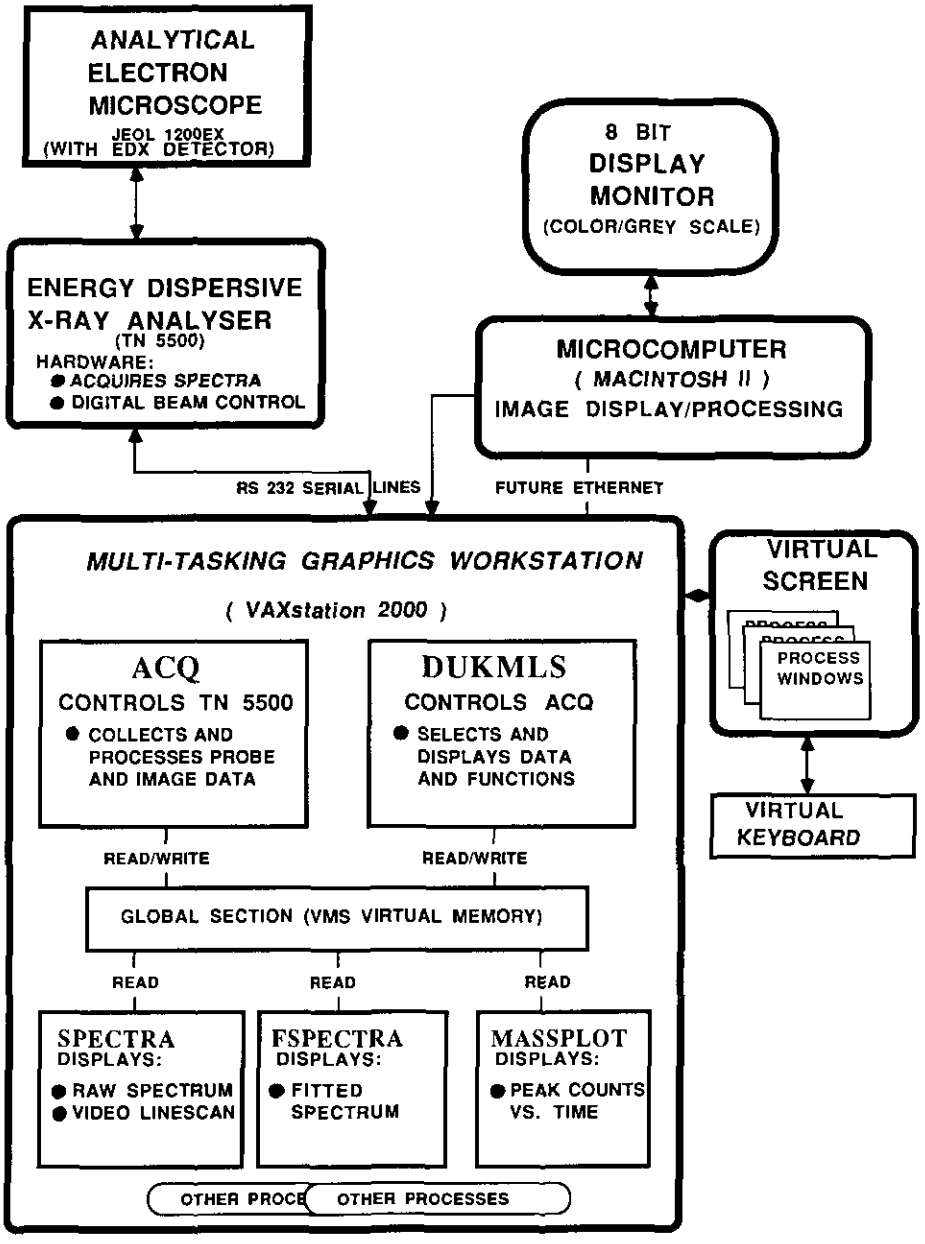

FIGURE 10. Schematic of a computer-controlled quantitative digital X-ray imaging system (*53,54*).

problem involves extracting reasonably good signal-to-noise ratios from very small peak-to-backgrounds that get progressively worse with increased specimen thickness (~60 nm in the case of biological tissue) due to multiple electron scattering. Moreover, the continuously sloping background makes deconvolution especially troublesome for some elements, such as phosphorus, in the presence of high amounts of organic material.

On the other hand, EELS is very sensitive to elements of low atomic number such as carbon, oxygen, and nitrogen, for which EPXMA is not usually satisfactory. However, since EELS can readily detect much lower energy events than EDX, it has been successfully used to measure elements, such as calcium, through transitions from the outer core electrons, i.e., the L-shell. The most important advantage of EELS lies in the potentially high spatial elemental resolution that can be obtained in a suitably configured instrument. Usually this requires using a field emission gun. Also it either requires digital scanning, where the EELS data at each pixel are processed quantitatively in a similar fashion to EDX digital imaging; or the placement of a magnetic prism in a conventional TEM, such that an energy filtered image is formed on film or a photoelectric device. In both instances, accurate subtraction of the background is crucial to avoid artifacts. Because of the processing difficulties alluded to above, this still remains a controversial area of research.

Energy loss spectra also contain a component of electrons that are either unscattered when they pass through the sample or scattered only elastically with

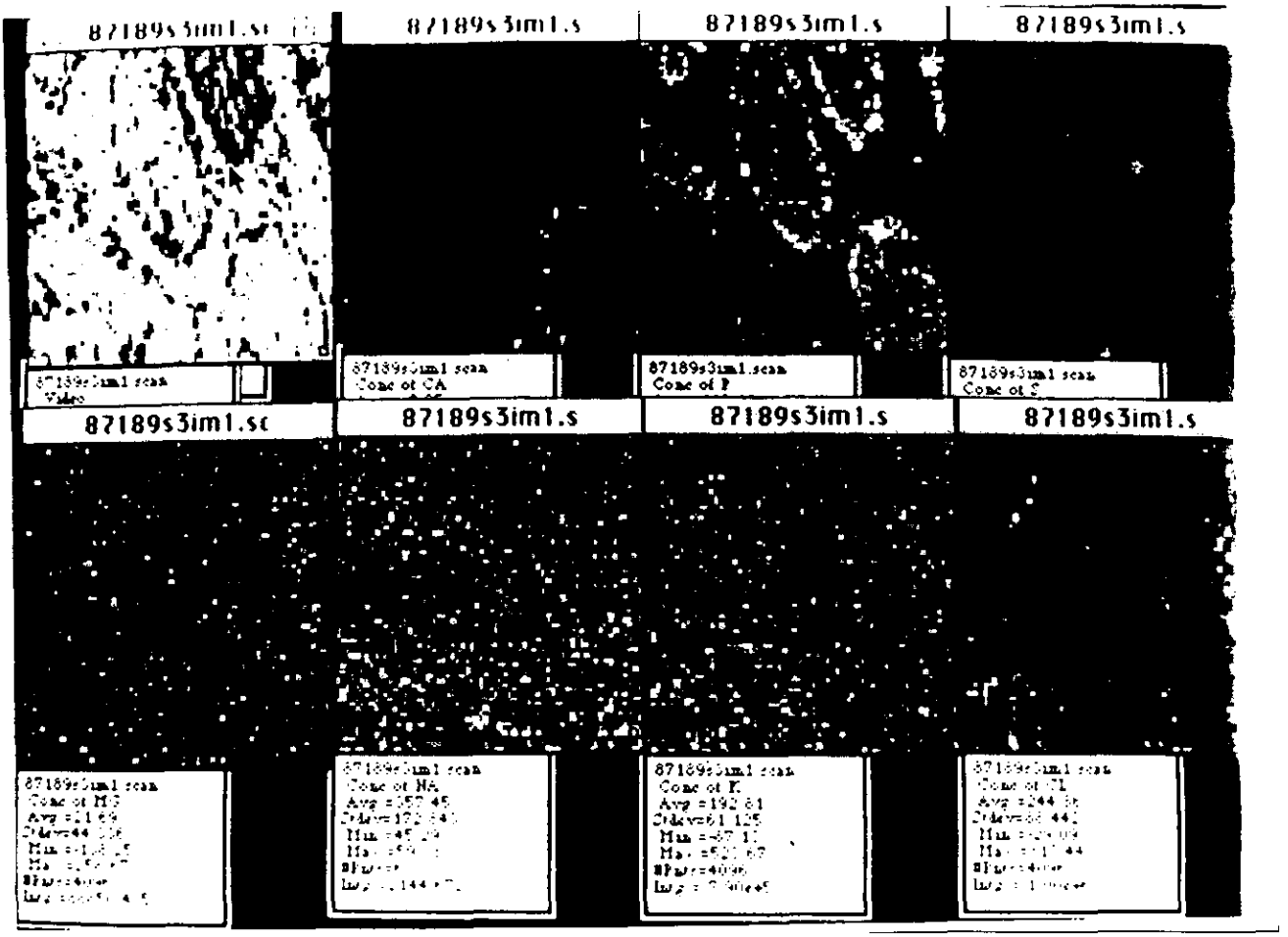

FIGURE 11. Quantitative energy dispersive X-ray maps (64 × 64 pixels) from quick-frozen, freeze-dried cryosection of human nasal epithelium. Magnification approximately × 3700.

no energy loss. In our laboratory (*21*) as well as others (*18*), significant potential has been realized for the use of zero-loss electrons in their proportionality to the mass thickness of the material. Ideally, localized microchemical information is required on the hydrated state of cells. This is especially important when comparisons are being made with physiological measurements from living cells and tissues. Quantitative mass thickness data/images can be obtained. These areas can be X-ray analyzed after freeze-drying. (The presence of ice usually undergoes radiolysis under the electron beam and absorbs too much of the X-ray signal to permit measurement of the low levels of physiologically important elements.) However, several other methods of measuring hydrated mass exist including acquiring other aspects of the normal transmitted image (*60*) as well as the backscattered electron signal (*61*).

Applications in Cell Physiology

Calcium has multiple effects on cell metabolism, membrane transport, and permeability and, thus, on overall cell physiology or pathophysiology. As Somlyo has succinctly stated, "Because cells can be frozen for X-ray microanalysis in various physiological states, it is possible to follow not only the movements of calcium within cells, but also the fluxes of counterions and/or co-ions that accompany redistribution" (*64*). While many examples of this powerful methodology are given in the literature (*62,63*), we present an overview of some initial results obtained in our laboratory on two experimental cell systems: cultured embryonic chick heart cells and a suspension of kidney proximal tubules, and one clinically related study using nasal epithelium from cystic fibrosis patients.

Fundamentals of Cell Preservation

Cells must be maintained (*1,7,55*) in a viable, physiologically defined state until the moment of cryopreservation (*62,63*). Cryopreservation (quick freezing) is the only satisfactory method by which both ultrastructure and intracellular diffusible element content can be simultaneously preserved. Freezing must occur at rates of approximately > 10,000°C/sec to approximately 100,000°C/sec, theoretically, without the formation of ice crystals (vitrification) or, practically, with the formation of ice crystals that are negligibly small in relation to the size of the regions to be

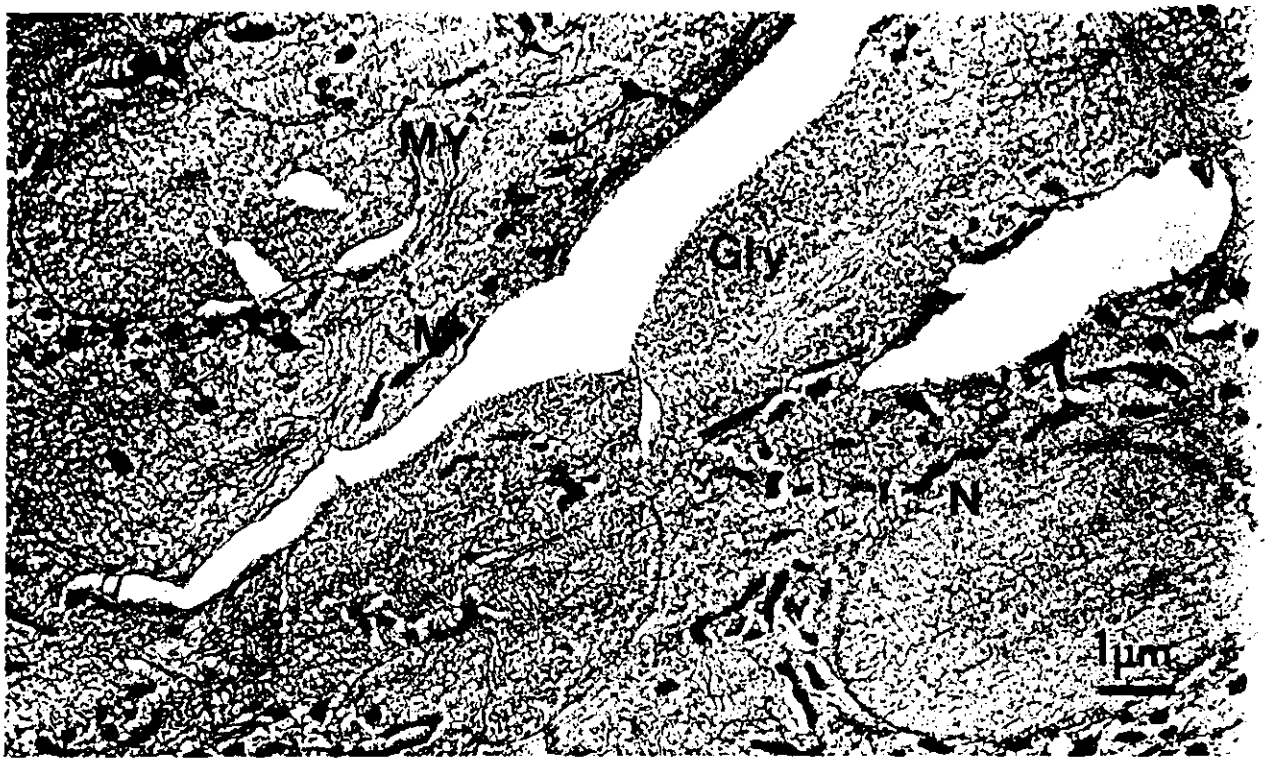

FIGURE 12. Transmission electron micrograph of quick-frozen, freeze-dried cryosection of cultured embryonic chick heart cells. No chemical fixatives or stains are used at any preparatory step. N, nucleus; M, mitochondria; Gly, glycogen; My, myofibrils. Magnification approximately 9900 ×.

analyzed. Many investigators agree that high resolution quantitative X-ray microanalysis of diffusible elements such as Ca must be performed on cells prepared by freezing, generally in the absence of additional penetrating cryoprotectants, chemical fixatives, or stains. Most embedding media and/or freeze-substitution techniques generate some form of chemical change in the cells or tissues. The reader should refer to numerous, excellent texts for details of the forementioned methodologies (*1,7,55,62,63*). Cryosectioning or other subsequent manipulation of the frozen, still-hydrated specimens must be performed at temperatures which preclude thawing and refreezing, nominally <-140°C. If analyses are made on freeze-dried specimens, then freeze drying either inside the microscope or in another vacuum device must be rigorously controlled so that water is removed at a rate that does not cause structural disruption or contamination. Precautionary measures should be taken to prevent rehydration of the sample with atmospheric moisture during either storage or transfer.

Experimental Cell Systems

Cultured Embryonic Chick Heart Cells. In studies of cultured embryonic chick heart cells, we implement, simultaneously, in the same preparation two methodologies, electron probe X-ray microanalysis and ion selective microelectrode (ISME) measurements, which allow correlation of element content and compartmental distribution with cytoplasmic ionic activity (*65*). In addition, the use of both EPXMA and ISME in the same preparation provides unique experimental data for evaluating methodological problems peculiar to each technique.

Heart cells are grown as 50 to 100 μm aggregates that beat synchronously and can be individually frozen for EPXMA as previously described (*65,66*). As illustrated in Figure 12, cryosections are obtained from frozen cells at <-140°C, freeze dried, and analyzed as described in the previous sections. Numerical results (Table 1) show the cell K:Na ratio to be 10–15 to 1 in cytoplasm and mitochondria. Calcium in both compartments is low, and there is no obvious sequestration of Ca within the mitochondria. Cytoplasmic calcium is qualitatively variable, suggesting that some X-ray probes include sarcoplasmic reticulum, a site of high calcium accumulation. Contents of the elements in mitochondria are lower on a dry weight basis than in

Table 1. Elemental content in cytoplasm and mitochondria of cultured embryonic chick heart cells as determined by EPXMA.

	mmole/kg dry weight						
	Na	Mg	P	S	Cl	K	Ca_2
Mitochondria	54	39	461	213	127	825	2.3
$n = 25$[a] SEM	7	3	17	8	19	44	1.7
Cytoplasm	92	64	527	200	134	1052	4.5
$n = 26$ SEM	13	6	34	18	26	87	1.9

[a] n = number of raster probes (500 sec) obtained from each region.

Table 2. Summary of intracellular concentrations of sodium, potassium, chlorine, and calcium in cultured embryonic chick heart cells.

	mM			
	Na	K	Cl	Ca
EPXMA[a] cytoplasm	12.5	143	20	0.7
ISME cytoplasm	8	140	37	—

[a]Conversion from EPXMA dry weight measurements (mmole/kg dry wt) made within cytoplasm to wet weight values is based on the assumption that cytoplasm is 85 to 90% (88%) hydrated.

Table 3. Ca content changes in heart cells induced by ØNA.[a]

Time after ØNa, min	Ca_{free},[b] μM	Ca_{tot},[c] nmole/mg protein	mM
0	0.070 ± 0.010	11.0 ± 1.0	1.47
20	0.165 ± 0.035	24.0 ± 2.0	3.21

[a]Values are means ± SE. Data from Murphy et al. (*67*).
[b]Free intracellular Ca concentration (Ca_{free}) measured using the fluorescent dye Quin-2.
[c]Total cell calcium content (Ca_{tot}) measured by atomic absorption spectrophotometry; 7.47 μL cell H_2O/mg protein.

paired regions of the cytoplasm; however, the greater number of X-ray continuum counts in mitochondria (~1900), as compared to the adjacent cytoplasm (~800), indicates that the mitochondria are less hydrated originally than the cytoplasm. Energy loss measurements of mass thickness of hydrated and freeze-dried cryosections demonstrate that mitochondria are approximately 65% hydrated and cytoplasm, 88 to 90% hydrated (*21*). These hydration values are essential for conversion of the dry weight content values obtained by EPXMA to wet weight concentrations. Thus, physiologically meaningful comparisons of ionic activity can be made with probe measurements of ion compartmentation, as illustrated in Table 2 for Na, K, and Cl. Cl concentration, as measured by ISME, is higher than the values obtained from EPXMA, coulometric, or isotope analyses. Cl activity has been corrected for HCO_3^-, but may be overestimated since liquid ion-exchange electrodes respond to other anions.

In a second series of experiments we are examining Na and Ca compartmentation as they relate to both the Na-Ca exchange and the Na-K-2Cl co-transport mechanisms identified by biochemical and electrophysiological means (*67-69*). As shown in Table 3, when the normal transmembrane Na gradient is reversed by incubation of cells in Na-free medium, cells rapidly accumulate Ca and loose Na. Free Ca increases, but not enough to account for the observed change in total calcium (Ca_{tot}), suggesting that Ca is compartmentalized (*67*). EPXMA of cells frozen following this treatment reveals that Na content in all compartments is below the level of detection at 20 min (Table 4) and falls to < 10% of control within 4 min. Ca content in cytoplasm (including sarcoplasmic reticulum) at 20 min is three times that in control and in mitochondria, two times that in control. Over this time course, K and Cl decrease. These initial data suggest that Na efflux occurs rapidly and uniformly from all compartments, while Ca influx or uptake is compartmentalized and variable between mitochondrial and cytoplasmic (including sarcoplasmic reticulum) compartments.

Kidney Proximal Tubule. The calcium content of mitochondria *in situ* is another biological problem that is uniquely and directly approachable by EPXMA. Considerable controversy has existed over the years as to whether mitochondria contain sufficient Ca to effectively regulate cytoplasmic free Ca via the mitrochondrial Ca efflux pathway, or whether mitochondrial calcium is very low and compatible with modulation of Ca-sensitive mitochondrial enzymes through small (micromolar) fluctuations in mitochondrial matrix free [Ca]. The source of this controversy to a large extent was the wide range of calcium concentrations measured in isolated mitochondria and the uncertainty of the effects of isolation on Ca content.

In the kidney, in particular, a very wide range of values has been reported for total cell and mitochondrial Ca content; therefore, we have utilized EPXMA

Table 4. Elemental content in nucleus, cytoplasm plus sarcoplasmic reticulum (SR), and mitochondria as determined by EPXMA.

Time after ØNa, min	Intracellular compartment	mmole/kg dry wt				
		n[a]	Na	K	Cl	Ca
0	Nucleus	6	135 ± 7	421 ± 23	106 ± 8	5.0 ± 3.0
	Cytoplasm +SR	37	120 ± 14	923 ± 73	131 ± 19	6.0 ± 2.0
	Mitochondria	36	79 ± 9	698 ± 45	114 ± 14	2.9 ± 1.0
20	Nucleus	10	4 ± 14	568 ± 29	77 ± 11	−1.9 ± 5.1 ND[b]
	Cytoplasm +SR	10	−16 ± 15 ND[b]	646 ± 50	106 ± 18	17.3 ± 6.8
	Mitochondria	10	−8 ± 12 ND[b]	348 ± 24	35 ± 7	7.2 ± 3.1

[a]n = number of raster probes (500 sec) obtained from each region; values are means ± SE.
[b]ND = not detectable.

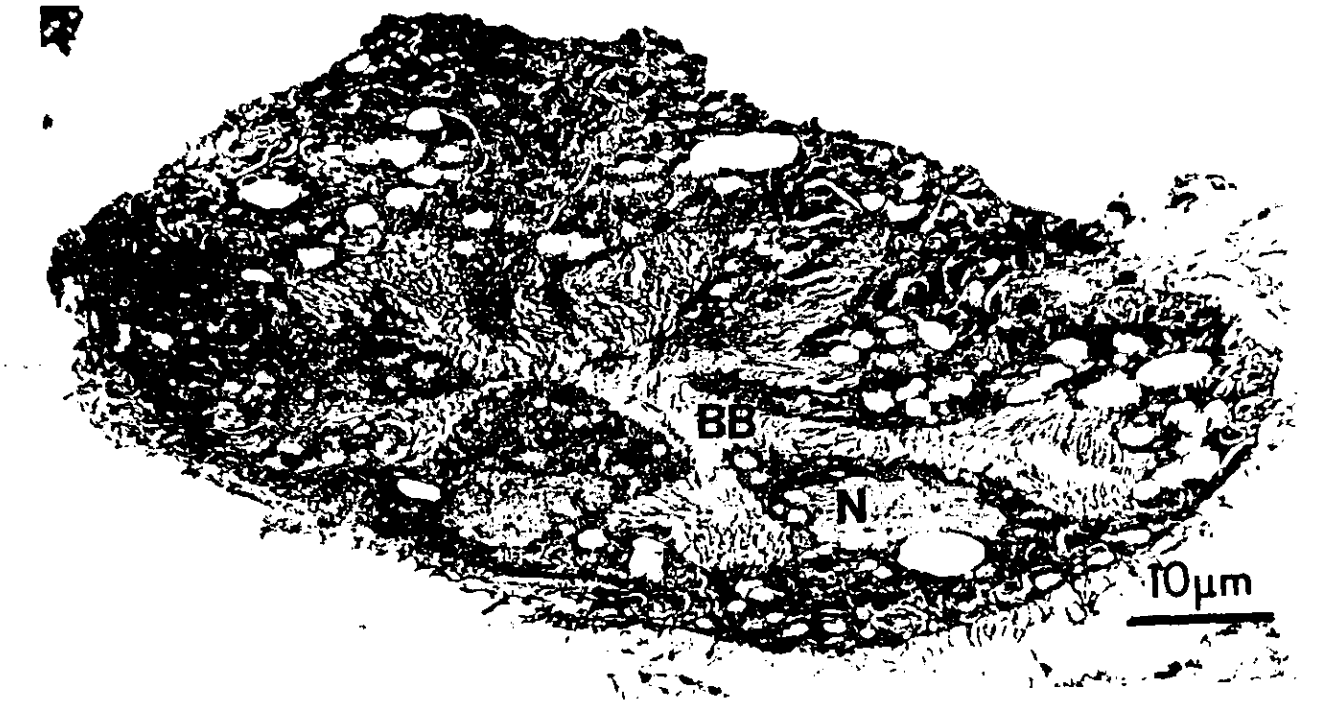

FIGURE 13. Transmission electron micrograph of quick-frozen, freeze-dried cryosection of rabbit kidney proximal tubule. (Magnification approximately 6300×). BB, brush border; M, mitochondria; N, nucleus.

to determine Ca content of the intracellular compartments in question (*68*). Proximal tubules are isolated from the rabbit kidney, rapidly frozen, and cryosectioned for EPXMA, as previously described (*68*). Tubule structure is well preserved by freezing with brush border, open lumen, and numerous mitochondria visible in cryosections (Fig. 13). Figure 14 illustrates quantitative digital X-ray images from two adjacent cells. Values from control preparations for all the elements are shown in Table 5, part A. Note K:Na is approximately 3 to 4:1 and Ca is low in both compartments, for an average cell Ca content of approximately 3.8 mmole/kg dry weight. A small proportion of non-viable cells have the element content as enumerated in Table 5, Part B; overall Ca content in such cells is approximately 210 mmole/kg dry weight. Average total cell Ca content of proximal tubule cell suspensions measured by atomic absorption spectrophotometry (AA) is approximately 13 mmole/kg dry weight; whole kidney tissues also range in Ca content from approximately 3 to 14 mmole/kg dry weight. These discrepancies could be accounted for if only 1 to 5% of cells were nonviable.

The EPXMA techniques combined with measurements of cytoplasmic-free Ca by fluorescent indicators are currently used to study the role of Ca in anoxic renal injury (*69,70*). Our results indicate that Na:K is 1:1, Cl is increased, and Ca is increased in the cytoplasm but not in mitochondria. One interpretation at this point is that the major buffering component resides in the cytoplasm, and this view is strengthened by the free Ca measurements which indicate no increase in free Ca during anoxia.

Table 5. Elemental contents in cytoplasm and mitochondria of kidney proximal tubules.[a]

	Elemental content, mmole/kg dry wt							
	Na	Mg	P	S	Cl	K	Ca	n^b
A. Viable cells								
Cytoplasm	125 ± 12	27 ± 4	356 ± 18	124 ± 8	141 ± 11	348 ± 23	4.1 ± 1.4	23
Mitochondria	95 ± 7	27 ± 3	349 ± 22	158 ± 6	131 ± 12	349 ± 22	3.1 ± 1.1	23
B. Nonviable cells								
Cytoplasm	261 ± 16	26 ± 5	288 ± 16	147 ± 14	70 ± 1-	206 ± 11	15 ± 2	9
Mitochondria	154 ± 29	37 ± 16	612 ± 85	112 ± 17	187 ± 23	124 ± 16	685 ± 139	10

[a]Data from LeFurgey et al. (*68*).
[b]n = number of 500-sec raster probes obtained from each region; values are means ± SE.

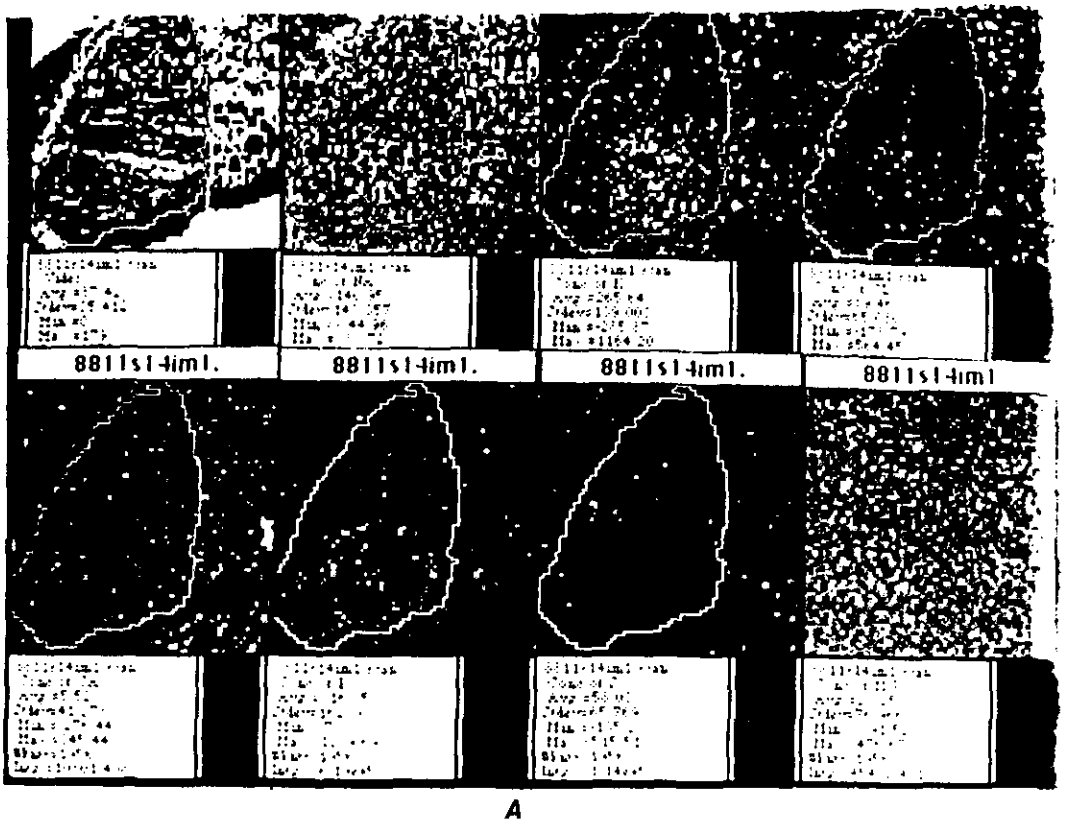

FIGURE 14. (*A*) Quantitative energy dispersive X-ray maps (64 × 64 pixels) from quick-frozen, freeze-dried cryosection of rabbit kidney proximal tubule. Outlined area is of normal morphology and shows expected cell element content. × 2800.

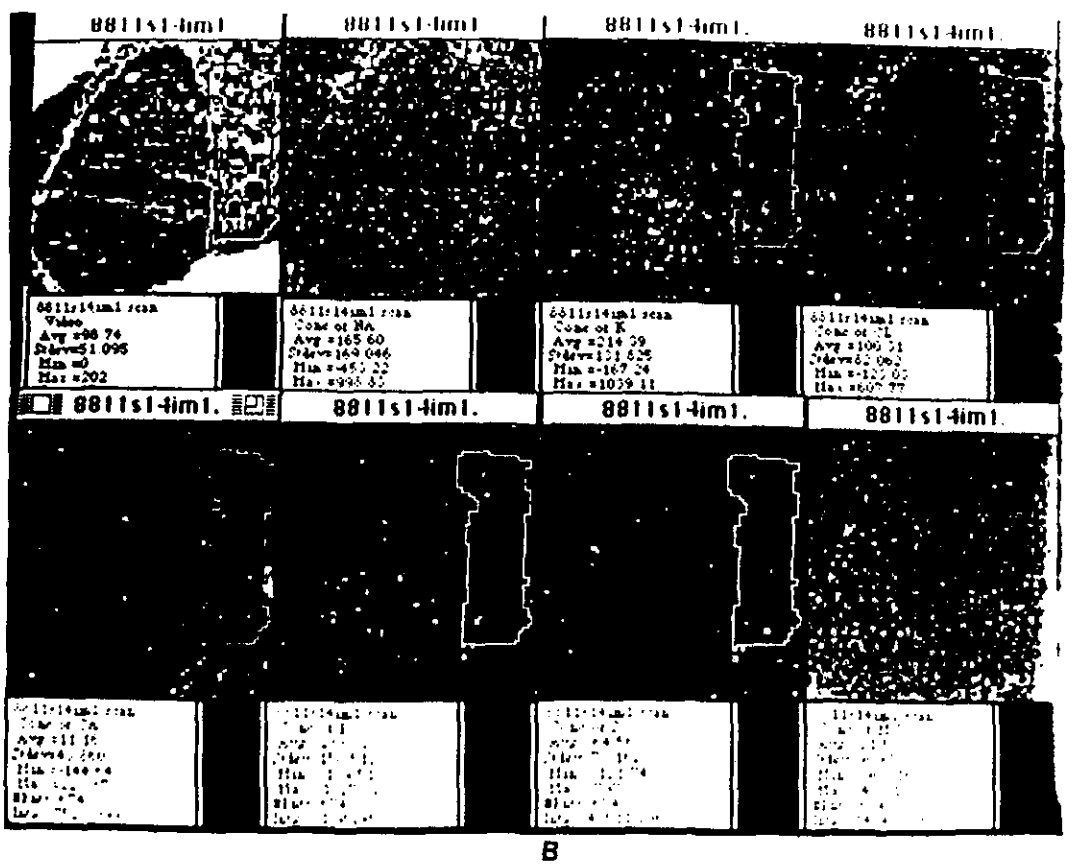

FIGURE 14. (*B*) Quantitative X-ray map from same proximal tubule as *A*. Outlined area is of altered morphology and shows different element concentrations typical of an injured cell. × 2800.

Clinical Pathophysiology: Nasal Epithelium/Cystic Fibrosis

The examples discussed thus far represent primarily the application of EPXMA to basic questions regarding the transport of diffusible elements and diffusible element compartmentation. EPXMA also has great potential for use at the clinical and toxicological level for qualitative diagnosis (*71*) of the presence of toxic elements, e.g., lead, arsenic, copper, etc. The procedure may also be used to characterize and/or diagnose diseases associated with altered membrane transport, for example cystic fibrosis, in which both Ca and Cl have been variously implicated as possible mediators of the disease process (*72*).

Quantitative elemental X-ray imaging expands the usefulness of EPXMA in these studies by providing both a statistically larger sample size and a greater ease of recognition of elemental compartmentation. Illustrated in Figure 11 are a representative scanning transmission image (video) and element images from a cryosection obtained from human nasal epithelium. Initial quantitative data from two patients with cystic fibrosis indicate that calcium and sulfur occur in mucous granules of these cells but at higher levels than in normal controls.

Summary

Our approach in investigating the role of Ca and other elements in cell physiology and pathophysiology is, of necessity, multidisciplinary. The maintenance of cell element/ion homeostasis involves complex interactions of metabolism, membrane transport, electrical properties, structure and element compartmentation. EPXMA is utilized for these latter two parameters, while both biochemical techniques for measuring free cytoplasmic and total cell ion contents and electrophysiological techniques for measuring ionic activities are performed in parallel on the same preparations. Our major physiological thesis is that X-ray microanalytical data are of enormous value for interpretation of cell function when utilized in conjunction with other techniques.

Our collaborators are gratefully acknowledged for their combined effort in establishing the Analytical Electron Microscopy Facility in the Department of Physiology, Duke University: Professors M. Lieberman, J. R. Sommer, L. J. Mandel, S. Simon, and J. D. Shelburne.

We also acknowledge the following people who made the physiological correlations possible by their active collaboration: R. Boucher and M. Knowles, UNC-CH; Elizabeth Murphy, NIEHS; Shi Liu and W. Jacobs, Duke University; and Rene Herlong, School of Medicine, Duke University.

D. Kopf and M. Lamvik provided help and advice with regard to energy loss analysis, and J. Costello, with regard to rapid freezing. We are indebted to A. V. and A. P. Somlyo and H. Shuman of the Pennsylvania Muscle Institute for sharing their quantitative computer routines and to S. Davilla for implementing them in our facility.

Larry Hawkey and Gay Gaster provided excellent technical and editorial skills in preparation of the manuscript. Supported in part by NIH grants HL-07101, HL-27105, DK-38820, DK-37704, HL-12486, and the VA Research Service.

REFERENCES

1. Somlyo, A. P. Cell calcium measurement with electron probe and electron energy loss analysis. Cell Calcium 6: 197-222 (1985).
2. Shuman, H, and Somlyo, A. P. Electron energy loss analysis of near trace element concentrations of calcium. Ultramicroscopy 21: 23-32 (1987).
3. Goldstein, J. I., Newbury, D. E., Echlin, P., Joy, D. C., Fiori, C.E., and Lifshin, E. Scanning Electron Microscopy and X-Ray Microanalysis. Plenum Press, New York, 1981, pp. 60-71.
4. Newbury, D. E., Joy, D. C., Echlin, P., Fiori, C. E., and Goldstein, J. I. Advanced Scanning Electron Microscopy and X-Ray Microanalysis. Plenum Press, New York, 1986, pp. 261-263.
5. Goldstein, J. I., Newbury, D. E., Echlin, P., Joy, D. C., Fiori, C. E., and Lifshin, E. Scanning Electron Microscopy and X-ray Microanalysis. Plenum Press, New York, 1981.
6. Hall, T. A., Echlin, P, and Kaufmann, R. (Eds.). Microprobe Analysis as Applied to Cells and Tissues. Academic Press, New York, 1974.
7. Hayat, M. A. (Ed.). X-Ray Microanalysis in Biology. University Press, Baltimore, MD, 1980.
8. Heinrich, K. F. J. Electron Beam X-Ray Microanalysis. Van Nostrand-Reinhold, Princeton, NJ, 1981.
9. Hren, J. J., Goldstein, J. I., and Joy, D. C. (Eds.). Introduction to Analytical Electron Microscopy. Plenum Press, New York, 1979.
10. Hren, J. J., and Ingram, P. (Eds.). Frontiers of Sub-micron Spectroscopy and Biological Microanalysis. Ultramicroscopy 24: 83-328 (1988).
11. Hutchinson, T. E., and Somlyo, A. P. (Eds.). Microprobe Analysis of Biological Systems. Academic Press, San Francisco, 1981.
12. Lechene, C. and Warner, R. (Eds.). Microbeam Analysis in Biology. Academic Press, New York, 1979.
13. Newbury, D. E., Joy, D. C., Echlin, P., Fiori, C. E., and Goldstein, J. I. Advanced Scanning Electron Microscopy and X-Ray Microanalysis. Plenum Press, New York, 1986.
14. Marshall, A. T. Principles and instrumentation. In: X-Ray Microanalysis in Biology (M. A. Hayatt, Ed.), University Park Press, Baltimore, MD, 1980, pp. 1-64.
15. Egerton, R. F. Electron Energy Loss Spectroscopy and Biology. Plenum Press, New York, 1986.
16. Colliex, C. Electron energy-loss spectroscopy analysis and imaging of biological specimens. Ann. N.Y. Acad. Sci. 483: 311-315 (1986).
17. Ottensmeyer, F. P. Elemental mapping by energy filtration: advantages, limitations, and compromises. Ann. N.Y. Acad. Sci. 483: 339-353 (1986).
18. Leapman, R. D., and Ornberg, R. L. Quantitative electron energy loss spectroscopy in biology. Ultramicroscopy 24: 251-268 (1988).
19. Jeanguillaume, C. Electron energy loss spectroscopy and biology. Scann. Mic. 1: 437-450 (1987).
20. Shuman, H., Chang, C. F., Buhle, E. L., Jr., and Somlyo, A. P. Electron energy-loss spectroscopy: quantitation and imaging. Ann. N.Y. Acad. Sci. 483: 295-310 (1986).
21. Kopf, D., LeFurgey, A., Hawkey, L. A., Craig, B., and Ingram, P. Mass thickness images of frozen hydrated and freeze dried sections. In: Microbeam Analysis—1986 (A. D. Romig and W. F. Chambers, Eds.) San Francisco Press, San Francisco, CA, 1986, pp. 241-244.
22. Garruto, R. M., Fukatsu, R., Yamagihara, R., Gjadused, D. C., Hook, G., and Fiori, C. E. Imaging of calcium and aluminum in neurofibrillary tangle-bearing neurons in Parkinsonism Dementia in Guam. Proc. Natl. Acad. Sci. (U.S.) 81:1875-1879 (1984).
23. Lechene, C., and Warner, R. Microbeam Analysis in Biology. Academic Press, New York, 1979.

24. Bonventre, J. V., Blouch, K., and Lechene, C. Liquid droplets and isolated cells. In: X-Ray Microanalysis in Biology (M. A. Hayatt, Ed.), University Park Press, Baltimore, MD, 1980, pp. 307-366.
25. Lechene, C. Electron-probe analysis of cultured cells. Ann. N.Y. Acad. Sci. 483: 270-283 (1986).
26. Marshall, A. T. Scanning electron microscopy and X-ray microanalysis of frozen-hydrated bulk samples. In: Cryotecniques in Biological Electron Microscopy (R. A. Steinbrecht and K. Zeirold, Eds.), Springer-Verlag, Berlin, 1987, pp. 240-257.
27. Shuman, H., Somlyo, A. V., and Somlyo, A. P. Quantitative electron probe microanalysis of biological thin sections: methods and validity. Ultramicroscopy 1: 317-339 (1976).
28. Fiori, C. E., Leapman, R. D., and Swyt, C. R. Quantitative X-ray mapping of biological cryosections. Ultramicroscopy 24: 237-250 (1988).
29. Kramers, H. A. Theory of X-ray absorption and of the continuous X-ray spectrum. Phil. Mag. 46: 836-871 (1923).
30. Russ, J. C. Selecting optimum KV for STEM microanalysis. In: Scanning Electron Microscopy, Vol. 1, 1977, pp. 335-340.
31. Bentley, J. Zaluzec, N. J., Kenik, E. A., and Carpenter, R. W. Optimization of an analytical electron microscope for X-ray microanalysis: instrumental problems. In: Scanning Electron Microscopy (O. Johari, Ed.), Vol. II, AMF O'Hare, IL, 1979, pp. 581-594.
32. Nicholson, W. A. P., Biddlecome, W. H., and Elder, H. Y. A low X-ray background low temperature specimen stage for biological microanalysis in the TEM. J. Microsc. 126: 307-316 (1982).
33. Zierold, K. X-ray microanalysis of freeze-dried and frozen-hydrated cryosections. J. Electron Microsc. Tech. 9: 57-64 (1988).
34. Bond, M., Vadasz, G., Somlyo, A. V., and Somlyo, A. P. Subcellular calcium and magnesium mobilization in rat liver stimulated in vivo with vaspressin and glucagon. J. Biol. Chem. 262: 15630-15636 (1987).
35. Hall, T. A. The microprobe assay of chemical elements. In: Physical Techniques in Biological Research (G. Oster, Ed.), 2nd ed., Vol 1A, Academic Press, New York, 1971, pp. 157-275.
36. Hall, T. A. Methods of quantitative analysis. J. Microscopie Biol. Cellulaire 22: (2-3), 271-82 (1975).
37. Hall, T. A. Reduction of background due to backscattered electrons in energy-dispersive X-ray microanalysis. J. Microsc. 117: 145-163 (1979).
38. Hall, T. A. Biological X-ray microanalysis. J. Microsc. 117: *145-163* (1979).
39. Hall, T. A. Problems of the continuum-normalization method for the quantitative analysis of sections of soft tissue. In: Microbeam Analysis in Biology (C. Lechene, and R. Warner, Eds.), Academic Press, New York, 1979, pp. 185-202.
40. Hall, T. A., and Gupta, B. L. Measurement of mass loss in biological specimens under an electron microbeam. In: Microprobe Analysis as Applied to Cells and Tissues (T. A. Hall, P. Echlin, and R. Kaufmann, Eds.), Academic Press, New York, 1974, pp. 147-158.
41. Hall, T. A., and Gupta, B. L. EDS quantitation and application to biology. In: Introduction to Analytical Electron Microscopy (J. J. Hren, J. I. Goldstein, and D. C. Joy, Eds.), Plenum Press, New York, 1979, pp. 169-97.
42. Hall, T. A., and Gupta, B. L. Quantification for the X-ray microanalysis of crysections. J. Microsc. 126: 333-345 (1982).
43. Kitazawa, T. H., Somlyo, A. P., and Shuman, H. Quantitative electron probe analysis: problems and solutions. Ultramicroscopy 11: 251-262 (1983).
44. Somlyo, A. V., Bond, M., Shuman, H., Somlyo, A. P. Electron - probe X-ray microanalysis of *in situ* calcium and other ion movements in muscle and liver. Ann. N.Y. Acad. Sci. 483: 229-240 (1986).
45. Rick, R., Dorge, A., and Thurau, K. Quantitative analysis of electrolytes in frozen dried sections. J. Microsc. 125: 239-247 (1982).
46. Bond, M., Shuman, H., Somlyo, A. P., Somlyo, A. V. Total cytoplasmic calcium in relaxed and maximally contracted rabbit portal vein smooth muscle. J. Physiol. 357: 185-201 (1984).
47. Bond, M., Kitazawa, T., Somlyo, A. P., and Somlyo, A. V. Release and recycling of calcium by the sarcoplasmic reticulum in guinea-pig portal vein smooth muscle. J. Physiol. 355: 677-695 (1984).
48. Somlyo, A. P. Compositional mapping in biology: X-rays and electrons. Ultrastructure Res. 88: 135-142 (1984).
49. Fiori, C. E. Quantitative compositional mapping of biological cryosections. Microbeam Analysis—1986: 183-186 (1986).
50. Chang, C. F., Shuman, H., and Somlyo, A. P. Electron probe analysis, X-ray mapping, and electron energy loss spectroscopy fo calcium, magnesium, and monovalent ions in log phase and in dividing *Escherichia Coli* B cells. J. Bacteriol. 167: 935-939 (1986).
51. Davilla, S. D., Ingram, P., LeFurgey, A., and Lamvik, M. Simple multiprocess data sharing with the VAX/VMS operation system. J. Electron Micros. Tech. 8: 227-228 (1988).
52. Davilla, S. D., Ingram, P., LeFurgey, A., and Lamvik, M. K. Real time graphic display of mass variation or elemental concentration during electron beam microanalysis using a general purpose computer. J. Microsc. 149: 153-157 (1988).
53. Ingram, P., LeFurgey, A., Davilla, S. D., Lamvik, M. K., Kopf, D. A., Mandel, L. J., and Lieberman, M. Real time quantitative elemental analysis and imaging in cells. Analytical Electron Microscopy—1987: 179-183 (1987).
54. Ingram, P., LeFurgey, A., Davilla, S. D., Sommer, J. R., Mandel, L. J., Lieberman, M., and Herlong, R. Quantitative elemental x-ray imaging of biological cryosections. Microbeam Analysis—1988: 433-439 (1988).
55. Johnson, D. E., Izutsu, K., Cantino, M., and Wong, J. High spatial resolution spectroscopy in the elemental microanalysis and imaging of biological systems. Ultramicroscopy 24: 221-236 (1988).
56. Saubermann, A. J., and Heyman, R. V. Quantitative digital X-ray imaging using frozen hydrated and freeze dried tissue sections. J. Microsc. 146: 169-182 (1987).
57. Lamvik, M. K., Ingram, P., Menon, R. G., Beese, L., Davilla, S. D., and LeFurgey, A. Correction for specimen movement after acquisition of element-specific electron microprobe images. J. Microsc., in press.
58. Kowarski, D. J. Intelligent interface for a microprocessor controlled scanning transmission electron microscope with X-ray imaging. J. Electron Microsc. Tech. 1: 175-184 (1984).
59. Statham, P. J. Quantitative digital mapping with drift correction. Analytical Electron Microscopy—1987, 187-190 (1987).
60. Zeitler, E., and Bahr, G. F. Contrast and mass thickness. Lab. Invest. 14: 208-216 (1965).
61. Niedrig, H. Electron backscattering from thin films. J. Appl. *Phys. 53: R15-R49 (1982).*
62. LeFurgey, A., Bond, M., and Ingram, P. Frontiers in electron probe microanalysis: application to cell physiology. Ultramicroscopy 24: 155-220 (1988).
63. Johnson, D. E. Analytical electron microscopy in the study of biological systems. Ann. N.Y. Acad. Sci. 483: 241-244 (1986).
64. Somlyo, A. P., and Somlyo, A. V. Electron probe analysis of calcium content and movements in sarcoplasmic reticulum, endoplasmic reticulum, mitochondria, and cytoplasm. J. Cardiovascular Pharmacol. 8(Suppl. 8): S42-S47 (1986).
65. LeFurgey, A., Hawkey, L. A., Lieberman, M., and Ingram, P. Quantitative elemental characterization of cultured heart cells by electron probe X-ray microanalysis and ion selective electrodes. Microbeam Analysis—1986, 205-208 (1986).
66. LeFurgey, A., Hawkey, L.A., Lieberman, M., and Ingram, P. Na-Ca compartmentation in cultured heart cells. Microbeam Analysis—1987: 267-268 (1987).
67. Murphy, E., Wheeler, D. M., LeFurgey, A., Jacob, R., Lobaugh, L. A., and Lieberman, M. Coupled socium-calcium transport in cultured chick heart cells. Am. J. Physiol. 250 (Cell Physiol. 19:) C442-C452 (1986).
68. LeFurgey, A., Mandel, L. J., and Ingram, P. Heterogeneity of calcium compartmentation: electron probe analysis of renal tubules. J. Membr. Biol. 94: 191-196 (1986).

69. LeFurgey, A., Mandel, L. J., Ingram, P., and Schreiner, P. Alterations in calcium compartmentation during anoxia in proximal renal tubules. Kidney Intern. 33: 361 (1988).
70. Jacobs, W. R., and Mandel, L. J. Role of cytosolic free calcium (Ca) in renal tubule damage during anoxia. Kidney Intern. 33: 359 (1988).
71. Ingram, P., Shelburne, J. D., and Roggli, V. (Eds.). Microprobe Analysis in Medicine. Plenum Press, New York, in press.
72. Herlong, J. R., LeFurgey, A., Ingram, P., Shelburne, J. D., Mandel, L. J., and Hawkey, L. A. Quantitative X-ray imaging of human cystic fibrosis nasal epithelium. Microbeam Analysis—1988: 447-450 (1988).